thermalization inside the bulk solid and e^+ being introduced externally at low energies. In any case, the interpretation of these effects in terms of pure metal surfaces is premature, and ultra-high-vacuum experiments are needed.

The photon counting system referred to in Fig. 1 is being employed in a search for 2430-Å photons resulting from the Lyman-α transition of the Ps if any is formed in the $n=2$ excited state.[12] If at least 0.1% of the Ps were formed in the $n=2$ state, we would observe a significant signal (95% confidence level) after a 24-h run with our present sensitivity. As of this writing, we have observed no Lyman-α photons for any target material investigated.

The authors wish to acknowledge valuable discussions regarding surface conditions with Dr. E. W. Plummer, University of Pennsylvania, and Dr. J. C. Tracy, General Motors Technical Center.

Note added.—The positronium formation has now also been confirmed by a direct 3γ coincidence measurement. Using an extended target chamber we obtain a triple coincidence rate between three 3×3-in. NaI(Tl) detectors, 10 cm from a Ti target, of 0.362 ± 0.027 sec^{-1} at 525°C versus 0.064 ± 0.013 sec^{-1} at 30°C with a background rate ≈0.017 sec^{-1}.

*Work supported by the National Science Foundation and the U. S. Army Research Office, Durham, N. C.

[1]P. G. Coleman, T. C. Griffith, and G. R. Heyland, Proc. Roy. Soc., Ser. A 331, 561 (1973).

[2]K. F. Canter, P. G. Coleman, T. C. Griffith, and G. R. Heyland, J. Phys. B: Proc. Phys. Soc., London 5, L167 (1972).

[3]W. C. Keever, B. Jaduszliwer, and D. A. L. Paul, in *Atomic Physics 3,* edited by S. J. Smith and G. K. Walters (Plenum, New York, 1973), p. 561.

[4]S. Pendyala, P. W. Zitzewitz, J. W. McGowan, and P. H. R. Orth, Phys. Lett. 43A, 298 (1973).

[5]D. G. Costello, D. E. Groce, D. F. Herring, and J. W. McGowan, Phys. Rev. B 5, 1433 (1972).

[6]R. Paulin and G. Ambrosino, J. Phys. (Paris) 29, 263 (1968).

[7]S. M. Curry and A. L. Schwalow, Phys. Lett. 37A, 5 (1971).

[8]R. Paulin, R. Ripon, and W. Brandt, Phys. Rev. Lett. 31, 1214 (1973).

[9]H. Kanagawa, Y. H. Ohtsuki, and S. Yanagawa, Phys. Rev. 138, A1115 (1965), and references therein.

[10]N. D. Lang and W. Kohn, Phys. Rev. B 3, 1215 (1971).

[11]S. Pendyala, D. M. Bartell, and J. W. McGowan, Bull. Amer. Phys. Soc. 18, 1505 (1973).

[12]L. W. Fagg, Nucl. Instrum. Methods 85, 53 (1970), and references therein. Recently two groups [S. L. Varghese, E. S. Ensberg, V. W. Hughes, and I. Lindgren, Bull. Amer. Phys. Soc. 18, 1503 (1972); S. L. McCall, Bull. Amer. Phys. Soc. 18, 1512 (1973)] have reported experiments to excite ground-state Ps to the $n=2$ state.

Raman Scattering from Coherent Spin States in *n*-Type CdS

R. Romestain,* S. Geschwind, and G. E. Devlin
Bell Laboratories, Murray Hill, New Jersey 07974

and

P. A. Wolff†
Department of Physics, Massachusetts Institute of Technology, Cambridge, Massachusetts 02139

(Received 8 May 1974)

When the donor spins in n-CdS are simultaneously irradiated with laser light at frequency ω_L and microwaves at frequency ω_0 near the spin resonance, intense sidebands at $\omega_L \pm \omega_0$ are observed for forward scattering which are more than 3 orders of magnitude greater than those for spontaneous spin-flip Raman scattering. This phenomenon is explained as Raman scattering from coherent states.

We have observed intense sideband radiation at frequencies $\omega_L \pm \omega_0$, when the electron spins in n-CdS are simultaneously irradiated with laser light at frequency ω_L and microwaves at frequency ω_0, close to the donor-spin resonance frequency. These huge sidebands are observed in the forward direction and are at least *3 orders of magnitude stronger than those due to spontaneous spin-flip Raman scattering* (SFRS). This effect has been seen in crystals ranging in concentration from (1 to 5)$\times10^{17}$ (excess donors)/cm^3. It may be described as coherent SFRS from coherent spin states or, alternatively, as parametric conversion of light via the macroscopic magnetic

dipole precessing at frequency ω_0. In optimal cases a conversion efficiency of 6% has been seen.

The experiment described below is a new type of optically detected EPR, which may prove advantageous in studying semiconductors in the Mott-transition regime, covered by our sample concentrations,[1] where EPR and relaxation measurements have been difficult.

The apparatus used to observe SFRS and simultaneously irradiate the sample with microwaves is similar to that previously used to study the microwave-phonon bottleneck with Brillouin scattering.[2] It was simply modified for observation of forward light scattering (as compared to 90° scattering) by use of a mirror as shown in Fig. 1(a). The laser beam—a single-mode Ar^+ at 4880 Å—propagates at a small angle θ relative to the c axis of the crystal. It should be emphasized, however, that the scattered light is viewed along the direction of the laser beam, as the coherent SFRS is collinear with the incident beam as will be discussed below.

Figure 1(a) shows the SFRS spectrum as analyzed by a piezoelectrically scanned Fabry-Perot interferometer in a sample with 2×10^{17} excess donors. The observed ratio of Stokes to anti-Stokes emission is in rough accord with the expected Boltzmann factor for a temperature of 2°K and a field of 9600 G. These measurements parallel earlier work on spontaneous SFRS in n-CdS.[3,4] Here, however, lower field and higher resolution are used.

Figure 1(b) illustrates the more than 3 orders of magnitude increase in forward sideband scattering that occurs when a resonant microwave field H_1 is applied to the sample. The observed difference in intensity between Stokes and anti-Stokes emission in Fig. 1(b), and its reversal when the polarization of the incident laser beam is rotated by 90°, as illustrated in Fig. 1(c), is due to phase-matching conditions detailed below. The larger peaks in Figs. 1(b) and 1(c) correspond to an intensity which is approximately 5% of the laser beam. The variation in intensity of the scattered light as the magnetic field is swept through its resonant value $H_0=\hbar\omega_0/g\mu_B$ reflects the EPR signal as discussed below. However, its frequency shift is always equal to the driving frequency ω_0.

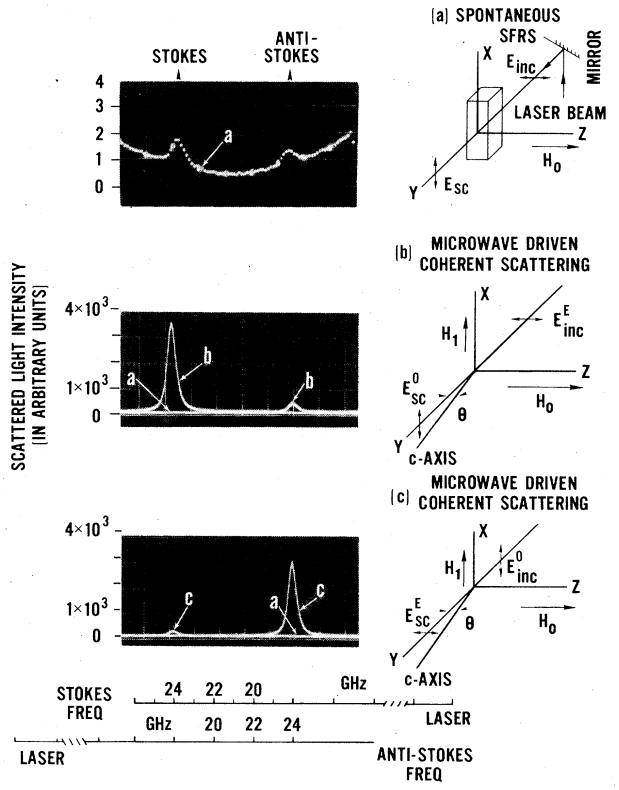

FIG. 1. Forward SFRS spectra at 2°K and associated geometries: (a) without resonant 23.96-GHz microwave excitation of the spins; (b) and (c) with microwave excitation (spectrum a is shown for comparison). The c axis is in the y-z plane. Depending upon whether E_L is in this plane (b) or perpendicular to it (c), phase matching favors Stokes or anti-Stokes emission, respectively. The other weak component is also seen as a result of depolarization of incident light.

The coherent effect described above may be calculated by following a semiclassical treatment. Raman scattering between two general states $|a\rangle$ and $|b\rangle$ may be viewed as radiation from a Raman dipole resulting from the admixture of excited states $|n\rangle$ into $|a\rangle$ and $|b\rangle$ via coupling to the electric field $\vec{E}_L\cos(\omega t)$ of the incident light beam. To lowest order in E_L, the modified ground states $|\psi_a\rangle$ and $|\psi_b\rangle$, with energies $\hbar\omega_a$ and $\hbar\omega_b$, respectively, may be written as[5]

$$|\psi_a\rangle=\exp(-i\omega_a t-i\varphi)\{|a\rangle-\tfrac{1}{2}\textstyle\sum_n|n\rangle[\langle n|\vec{E}_L\cdot e\vec{r}|a\rangle/(E_n-E_a-\hbar\omega_L)]\exp(-i\omega_L t)\}. \quad (1)$$

For simplicity we have dropped the nonresonant term in $|\psi_a\rangle$ as the frequency of the laser light is close to an intermediate-state resonance. $|\psi_b\rangle$ is given by an equation similar to (1) with b replacing a, but without the factor $e^{-i\varphi}$, which describes the relative phase between the states and is random

for spontaneous scattering.

It is convenient to introduce an effective Raman dipole operator $\vec{D}^{(2)}$ which operates in the two-dimensional manifold of the unperturbed states $|a(t)\rangle = |a\rangle \exp(-i\omega_a t - i\varphi)$ and $|b(t)\rangle = |b\rangle \exp(-i\omega_b t)$ such that

$$\langle \psi_b(t)| e\vec{r} |\psi_a(t)\rangle = \langle b(t)| \vec{D}^{(2)} |a(t)\rangle. \tag{2}$$

In most general fashion any such operator may be expressed in terms of a fictitious spin $S=\frac{1}{2}$ formalism.[6] Thus

$$D_k^{(2)} = \sum_{ij} \alpha_{ijk} E_{Li} \sigma_j \exp(-i\omega_L t) + \beta_{ik} E_{Li} \tilde{I} \exp(-i\omega_L t) + \text{c.c.}, \tag{3}$$

where the σ_j's are the Pauli matrices and where we have taken $E_n - E_a \simeq E_n - E_b$. For the case where $|a\rangle$ and $|b\rangle$ are time-reversed states split by a magnetic field along z and for cubic symmetry,[7] it follows easily that

$$\vec{D}^{(2)} = \vec{\sigma} \times \vec{E}_L [\alpha \exp(-i\omega_L t) + \text{c.c.}] + [\beta \vec{E}_L \tilde{I} \exp(-i\omega_L t) + \text{c.c.}], \tag{4}$$

where[8]

$$\alpha = \sum_n \tfrac{1}{2} i \langle a|ex|n\rangle\langle n|ez|b\rangle / (E_n - E_a - \hbar\omega_L). \tag{5}$$

In Eq. (4), β corresponds to the usual polarizability which gives rise to the Rayleigh scattering. Interaction of $\vec{D}^{(2)}$ with the Raman-scattered light $\vec{E}_R$ immediately yields the effective spin-flip Hamiltonian,

$$\mathcal{H}_{sf}^{(2)} = \tfrac{1}{2} \alpha \vec{\sigma} \cdot (\vec{E}_L \times \vec{E}_R) \exp[-i(\omega_L - \omega_R)t] + \text{c.c.}, \tag{6}$$

previously used to describe spontaneous SFRS in semiconductors[9] and the parametric generation in the far infrared by the mixing of two laser beams.[10]

Spontaneous Raman scattering between $|a\rangle$ and $|b\rangle$ is associated with the Raman electric dipole,

$$\langle b(t)| \vec{D}^{(2)} |a(t)\rangle = \exp(+i\omega_{ba} t - i\varphi)[\alpha \exp(-i\omega_L t) + \text{c.c.}] \langle b|\vec{\sigma}|a\rangle \times \vec{E}_L. \tag{7}$$

The appropriate dipole to use in the classical radiation formula is $\langle b(t)|\vec{D}^{(2)}|a(t)\rangle + \text{c.c.}$, where for Stokes emission one omits the energy nonconserving term $\exp[+i(\omega_L + \omega_{ba})t]$. Similarly, for anti-Stokes emission one omits the $\exp[+i(\omega_L - \omega_{ba})t]$ term. Radiation in the transverse plane of this dipole can be expressed in terms of a spontaneous differential Raman cross section per center, given by

$$(d\sigma/d\Omega)_{sp} = 4|\alpha|^2 (\omega_L \pm \omega_{ba})^4 / c^4. \tag{8}$$

The important point to be emphasized is the random-phase factor φ in Eq. (7) which results in the incoherent spontaneous Raman scattering from the centers. By contrast, we now consider the case where the system is prepared as a coherent superposition of states $|a\rangle$ and $|b\rangle$ as is done in our experiment by application of a coherent microwave field of frequency ω_0 near resonance with ω_{ba}, i.e.,[11]

$$c(t) = \lambda |a\rangle + \mu \exp(i\omega_0 t) |b\rangle. \tag{9}$$

λ and μ are related to the components of $\langle\vec{\sigma}\rangle$ which are in turn given by solutions to the Bloch equations,[12] neglecting the feedback of the Raman light. The magnitude of the transverse component of precessing magnetization is $\sigma_T = \frac{1}{2}|\lambda\mu|$. By the use of (4) and (9), it is seen that the state $|c(t)\rangle$ displays an oscillating Raman dipole,

$$\vec{D}_{cc}^{(2)} = \langle c(t)|\vec{D}^{(2)}|c(t)\rangle = [\lambda\mu^* \langle a|\vec{\sigma}|b\rangle \times \vec{E}_L \exp(-i\omega_0 t) + \text{c.c.}][\alpha \exp(-i\omega_L t) + \text{c.c.}]. \tag{10}$$

All dipoles in Eq. (10) have their phase unambiguously defined in contrast to spontaneous scattering [Eq. (7)]. These coherent electric dipoles constitute a superradiant source in the Dicke sense[13] which will emit cooperatively in the forward direction at frequencies $\omega_L \pm \omega_0 = \omega_S$ provided that a phase-matching condition $\Delta k = k_L - k_S - k_0 = 0$ is fulfilled, or $k_L - k_S \simeq 0$ since the microwave frequency corresponds to $k_0 \simeq 0$. It should be noted that emission depends on σ_T and will therefore persist for the phase memory time T_2 of σ_T even after the microwaves are removed.

Using $\eta \ddot{D}_{cc}^{(2)}$ as a source term in Maxwell's

equations, one has for the geometry shown in Fig. 1

$$2ik_S\left(\frac{\partial E_S}{\partial y}+\frac{\gamma}{2}E_S\right)\simeq-\frac{4\pi\omega^2}{c^2}D_{cc}^{(2)}\eta e^{i\Delta ky}. \qquad (11)$$

Here E_S is the sideband field amplitude, k_S the sideband wave vector, γ the absorption coefficient, and η the concentration. Note that $D_{cc}^{(2)}$ has the factor $e^{-\gamma y/2}$ via E_L. Equation (11) can be integrated to estimate P_S/P_0, the ratio of intensities of Raman to laser light exiting from the crystal. The factor α appearing in $D_{cc}^{(2)}$ can be expressed in terms of $(d\sigma/d\Omega)_{sp}$ via Eq. (8), giving

$$\frac{P_S}{P_0}=\frac{1}{2}\left(\frac{d\sigma}{d\Omega}\right)_{sp}\frac{\lambda_s^2\eta^2\sigma_T^2}{\epsilon}\frac{1-\cos(\Delta kL)}{\Delta k^2}, \qquad (12)$$

where λ_s is the free-space optical wavelength, ϵ the optical dielectric constant, and L the interaction length ($L=1$ mm). From the measured values of T_1 and T_2 given below, we estimate $\sigma_T^2\simeq 3\times10^{-5}$. $d\sigma/d\Omega\simeq10^{-19}$ cm^2 for 4880 Å light in moderately doped n-CdS[3,4] with $\eta=2\times10^{17}$. Thus, $P_S/P_0\simeq0.08$ for our sample, in reasonable agreement with experiment, considering the large uncertainties in several of the quantities appearing in the numerical calculations.

As ω_L is very close to the band gap, one cannot neglect the dispersion $d=\pm(\partial k/\partial\omega)\omega_0$, in attempting to satisfy $\Delta k=0$, even though ω_0 is only as small as 0.8 cm^{-1}. However, since according to the selection rules of Eq. (11) $\vec{E}_L\perp\vec{E}_S$, this dispersion may be compensated for by the birefringence $b(\theta)$ of the uniaxial CdS crystal, which for propagation at angle θ close to the c axis may be expressed as $b(\theta)\simeq(n_0-n_E)\theta^2$. The birefringence cancels the dispersion when $\theta=[d/(k_0-k_E)]^{1/2}$, *provided the higher-frequency wave propagates as an extraordinary wave.* Using $d=5\times10^{-4}$ [14] and our measured value of $n_0-n_E=0.22$, one finds $\theta\simeq3°$ in agreement with observation within experimental error. At this angle, the Stokes generation is phase matched if $\vec{E}_L$ is in the extraordinary polarization [Fig. 1(b)]. If $\vec{E}_L$ is changed to ordinary, the intensities should reverse [Fig. 1(c)].

When the dc magnetic field is swept through resonance, the intensity of the coherent SFRS sidebands reflects a nonconventional EPR signal. In most EPR experiments, one observes a signal proportional to either of the transverse components of spin in the rotating frame, $S_{x'}$ or $S_{y'}$, which are, respectively, in phase or out of phase with the rotating microwave field. In contrast,

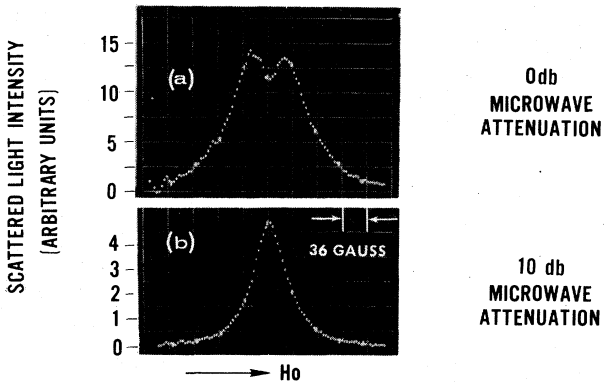

FIG. 2. Magnetic-field dependence of the intensity of the coherent Raman scattering. The resonance field corresponds to $g_\perp=1.77$. The broadening and dip at full power (a) indicates that the unsaturated EPR line, (b) is homogeneous with $T_2=4\times10^{-9}$ sec.

the signal we observe is proportional to $\sigma_T^2=S_{x'}^2+S_{y'}^2$. This distinction becomes quite marked in the saturation of the EPR line when $\lambda_e H_1(T_1T_2)^{1/2}>1$, at which point a double peak appears in σ_T^2 as seen in Fig. 2(a).

Transient microwave studies, to be reported later, on these signals have yielded a value of $T_1=5\times10^{-6}$ sec for a sample with $\eta=2\times10^{17}$ donors. A detailed analysis of the saturation behavior of σ_T^2, as displayed in Fig. 2(a), shows that the line is indeed homogeneous with $T_2=4\times10^{-9}$ sec. This short value of T_2 may be caused by loss of phase memory from exchange flipping between donors, or electron hopping at the onset of the Mott transition. Such unequal values of T_1 and T_2 in a hopping regime are contrary to the often-made assumption of $T_1=T_2$ in this regime.

We wish to thank P. A. Fleury, J. A. Giordmaine, P. Hu, S. L. McCall, L. R. Walker, and Y. Yafet for many helpful discussions and S. Bortas for polishing of the CdS samples.

---

*On leave from Centre National de la Recherche Scientifique, France.

†Research sponsored by the U. S. Air Force Office of Scientific Research, Air Force Systems Command, under Contract/Grant No. AFOSR 71-2010.

[1]S. Toyotomi and K. Morigaki, J. Phys. Soc. Jpn. 25, 807 (1968).

[2]W. J. Brya, S. Geschwind, and G. E. Devlin, Phys. Rev. B 6, 1924 (1972).

[3]D. G. Thomas and J. J. Hopfield, Phys. Rev. 175, 1021 (1968).

[4]J. F. Scott, T. C. Damen, and P. A. Fleury, Phys.

Rev. B 6, 3856 (1972).
[5]A. S. Davydov, *Quantum Mechanics* (Pergamon, New York, 1965), p. 316.
[6]See for example Sect. II of the paper by M. Blume, S. Geschwind, and Y. Yafet, Phys. Rev. 181, 478 (1969).
[7]While the noncubicity of CdS modifies the selection rules given by Eq. (4) (see Ref. 3), it has a small effect on our subsequent computation of the sideband power.
[8]Spin-orbit interaction is implicit in the wave functions $|n\rangle$. See Ref. 3 and Y. Yafet, Phys. Rev. 152, 855 (1956).
[9]Yafet, Ref. 8.
[10]T. L. Brown and P. A. Wolff, Phys. Rev. Lett. 29, 362 (1972); V. T. Nguyen and T. J. Bridges, Phys. Rev. Lett. 29, 359 (1972).
[11]Raman scattering from coherent states prepared by different techniques where the coherence was at the natural frequency of the system rather than a driving frequency, as in our case, has been described by J. A. Giordmaine and W. Kaiser, Phys. Rev. 144, 676 (1966); R. G. Brewer and E. L. Hahn, Phys. Rev. A 8, 464 (1973).
[12]A. Abragam, *Principles of Nuclear Magnetism* (Oxford Univ. Press, Oxford, England, 1961), pp. 44 ff.
[13]R. H. Dicke, Phys. Rev. 93, 99 (1954).
[14]K. F. Rodgers, Jr., unpublished.

Molecular Theory of Orientational Fluctuations and Optical Kerr Effect in the Isotropic Phase of a Liquid Crystal

C. Flytzanis and Y. R. Shen*
Laboratoire d'Optique Quantique, Centre National de la Recherche Scientifique, 91405 Orsay, France
(Received 28 February 1974)

By use of Kubo's statistical formalism, we show that the orientational fluctuations of interacting molecules are responsible for both the narrow central component and the broad Rayleigh-wing component in the light-scattering spectrum of a liquid crystalline material. The same formalism also describes the optical Kerr effect. We also point out the difference between the microscopic and the macroscopic order parameters.

The spectrum of light scattering from an isotropic nematic substance has a narrow central component presumably arising from fluctuations of the order parameter.[1] The order parameter here describes the orientational order of the long molecules in the medium.[2] On the other hand, a much broader central component was also observed in the spectrum.[3] Such a component always exists in ordinary liquids and is often called the Rayleigh-wing component.[4] It is well known that the Rayleigh-wing component comes from orientational fluctuations of molecules.[4] Thus, from the microscopic point of view, both components appear to be due to orientational fluctuations of molecules. It is then interesting to see how the orientational fluctuations can give rise to two very different components in the spectrum and how they are related. In this paper, we show from microscopic derivations that interaction between molecules is responsible for the observed results, and, in particular, the narrow central component appears because of the large mean-field modification on the orientational motion near a phase transition.

The orientational fluctuations are also directly related to the optical Kerr effect as a result of molecular reorientation.[5] From Kubo's fluctuation-dissipation theory,[6] we can express the birefringence induced by a linearly polarized optical field of sinusoidally varying intensity, $|E_0|^2(t) = |\mathcal{E}_0|_\Omega^2 \exp(-i\Omega t)$, in the isotropic phase as

$$\delta n(\Omega) = (2\pi/n) F(\Omega) |\mathcal{E}_0|_\Omega^2,$$
$$F(\Omega) = \delta\chi(\Omega)/|\mathcal{E}_0|_\Omega^2 = \beta\langle\delta\chi(0)\delta\chi(0)\rangle + i\Omega\beta\int_0^\infty \langle\delta\chi(0)\delta\chi(t)\rangle e^{-i\Omega t}\, dt, \tag{1}$$

where $\beta \equiv 1/kT$, $\delta\chi(t)$ is the anisotropy in the susceptibility induced by the field, and the angular brackets indicate the ensemble average. On the other hand, the average induced anisotropy of the polarizability for each molecule is

$$\delta\alpha(\Omega) = f(\Omega)|\mathcal{E}_0|_\Omega^2, \quad f(\Omega) = (\Delta\alpha) Q(\Omega)/|\mathcal{E}_0|_\Omega^2,$$
$$Q(\Omega) = [\beta\langle S(0)S(0)\rangle + i\Omega\beta\int_0^\infty \langle S(0)S(t)\rangle e^{-i\Omega t}\, dt](2\Delta\alpha/3N)|\mathcal{E}_{loc}|_\Omega^2 = \gamma(\Omega)|\mathcal{E}_{loc}|_\Omega^2, \tag{2}$$

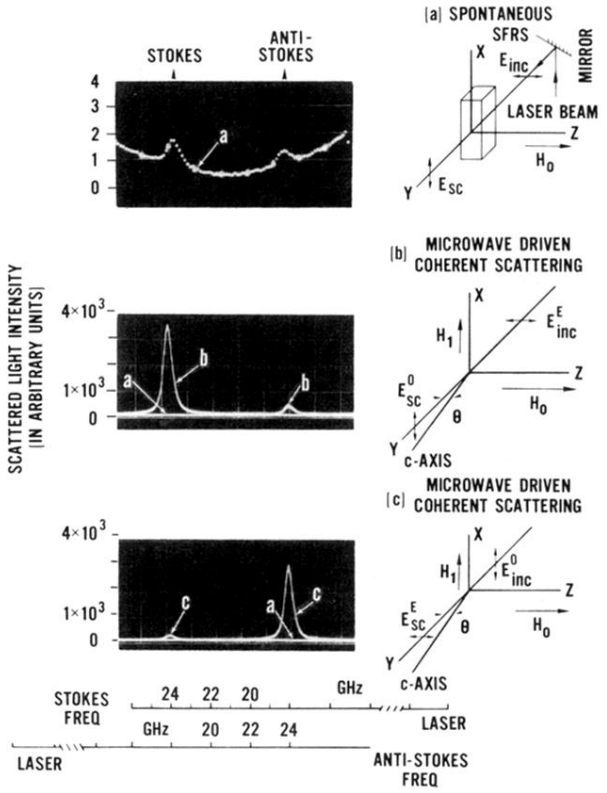

FIG. 1. Forward SFRS spectra at 2°K and associated geometries: (a) without resonant 23.96-GHz microwave excitation of the spins; (b) and (c) with microwave excitation (spectrum *a* is shown for comparison). The *c* axis is in the *y*-*z* plane. Depending upon whether E_L is in this plane (b) or perpendicular to it (c), phase matching favors Stokes or anti-Stokes emission, respectively. The other weak component is also seen as a result of depolarization of incident light.

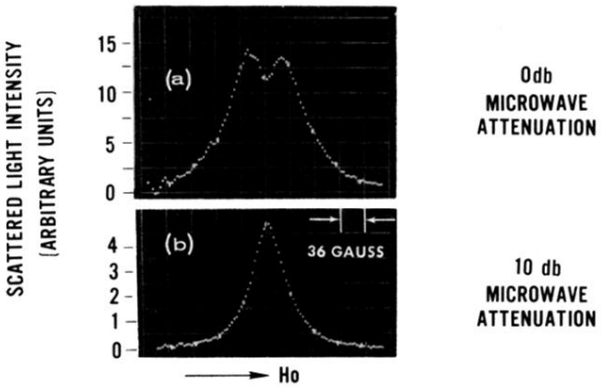

FIG. 2. Magnetic-field dependence of the intensity of the coherent Raman scattering. The resonance field corresponds to $g_{\perp}=1.77$. The broadening and dip at full power (a) indicates that the unsaturated EPR line, (b) is homogeneous with $T_2=4\times10^{-9}$ sec.